Finite Volume Method for Flow Prediction Using Unstructured Meshes

Juhee Lee, Yongjun Lee

Abstract—In designing a low-energy-consuming buildings, the heat transfer through a large glass or wall becomes critical. Multiple layers of the window glasses and walls are employed for the high insulation. The gravity driven air flow between window glasses or wall layers is a natural heat convection phenomenon being a key of the heat transfer. For the first step of the natural heat transfer analysis, in this study the development and application of a finite volume method for the numerical computation of viscous incompressible flows is presented. It will become a part of the natural convection analysis with high-order scheme, multi-grid method, and dual-time step in the future. A finite volume method based on a fully-implicit second-order is used to discretize and solve the fluid flow on unstructured grids composed of arbitrary-shaped cells. The integrations of the governing equation are discretised in the finite volume manner using a collocated arrangement of variables. The convergence of the SIMPLE segregated algorithm for the solution of the coupled nonlinear algebraic equations is accelerated by using a sparse matrix solver such as BiCGSTAB. The method used in the present study is verified by applying it to some flows for which either the numerical solution is known or the solution can be obtained using another numerical technique available in the other researches. The accuracy of the method is assessed through the grid refinement.

Keywords—Finite volume method, fluid flow, laminar flow, unstructured grid.

I. INTRODUCTION

THE characteristic of industrial applications is the geometrical complexity of interesting domains and therefore, the use of unstructured meshes for computational fluid analysis has become general. The main reason for this is the ability of unstructured meshes to discretize arbitrary and complex domains and the ease of local and adaptive grid refinement which enhances the efficiency of the solution as well as solution accuracy. In addition, solution algorithms for computing flows on unstructured grids have been continuously developed. Among the discretization methods, the finite volume methods (FVM) are most widely used for computational fluid dynamic (CFD) applications. This is mainly due to the inherent conservativeness of FVM and ease of understanding. These FVMs are capable to accommodate arbitrary polyhedral grids composed of cells of various topologies.

Muzaferija [1] developed a numerical code to improve the efficiency of CFD calculations in complex geometries encountered in wide engineering problems. The approach is to enable solutions free from the numerical error to be achieved economically by employing local mesh refinement to resolve regions of steep gradients, and using a multi-grid method to accelerate the convergence of the basic iterative solution technique. In order to identify regions requiring local refinement, and to assure the quality of the numerical solution, it was necessary to devise and investigate the use of error indicators.

Recently, Lestari [2] has developed and implemented the unsteady algorithms for incompressible Navier-Stokes flow on triangular unstructured grids. Three time integration methods such as a fully-implicit, Crank-Nicolson and an explicit four-step Runge-Kutta method use. A vertex-centered discretization with median-dual control volume is used and the equal order velocity pressure interpolation method is chosen to avoid the checkerboard problem in pressure commonly encountered in using a collocated grid. The numerical algorithm used to solve the resulting equations is derived from the SIMPLER algorithm. The Runge-Kutta SIMPLER uses the four-stage Runge-Kutta to update the velocities directly without a pressure correction equation in addition to fully implicit and Crank-Nicholson methods. The Runge-Kutta scheme is observed to perform well on low Reynolds number cases, but it becomes more unstable at higher Reynolds number, with the necessity of a finer grid density and lower time step.

Hadzi [3] has developed a fully-implicit second-order FVM to solve the unsteady fluid-flow equations on unstructured grids. Computational points are located in the cell center and a collocated variable arrangement is used. A segregated solution procedure is employed to solve the resulting set of non-linear algebraic equations. It leads to a decoupled system of linear algebraic equations for each dependent variable. The linearized equation systems are solved using a conjugate gradient solver. The SIMPLE algorithm, leading to an equation for the pressure correction, is used to establish the pressure-velocity coupling, calculate the pressure, and update the velocity filed to satisfy the continuity constraint.

Mathur and Murthy [4] have developed a pressure-based finite-volume scheme for unstructured meshes. The method admits arbitrary convex polyhedral meshes, including meshes with hanging nodes. Cell-based, collocated storage is used and discretization operators for the convective and diffusive fluxes are formulated so as to reduce to the well-known forms on body-fitted structured grids. Higher-order fluxes as well as secondary diffusion terms are computed using linear reconstruction and limiting similar to methods used for compressible flows. To minimize storage requirements, a

Juhee Lee is with Hoseo University, Asan, 31499, Korea (corresponding author to provide phone: +82-41-540-9669; fax: +82-41-540-9548; e-mail: juheelee@hoseo.edu).

Yongjun Lee is with the BEL technology, Seoul, 05542, Korea. (e-mail: ljyr1@naver.com).

segregated solution strategy is favored, with pressure and velocity coupled using the SIMPLE algorithm. An algebraic multigrid solver is used for the solution of linearized equations.

Unstructured grid methods have been the focus of a considerable amount of CFD research over the last a few decays. Engineers and scientists are interested in various phenomena of fluid flow in a complex geometry. A single numerical code for CFD is not fully satisfied the all of the requirements and thus, a number of CFD codes have been developed. In the middle of developing a new CFD code to calculate the natural convection phenomena next to the window cavity in the near future, we have implemented a code based on the SIMPLE method [5] for solving three-dimensional incompressible flow using unstructured grids. To validate the numerical methods, two validation calculations of lid-driven cavity and back-ward step flow are performed and the comparison shows the numerical methods implemented properly.

II. GOVERNING EQUATION

A. Reynolds Transportation Equation

The conservation equations for mass and momentum are used in their integral form for the numerical method. In terms of control volume method with arbitrary and unstructured meshes, the conservation equations are given in the coordinate-free form and the momentum equation is resolved in terms of Cartesian vector components. The conservation of a certain flow quantity means that its variation inside a control volume can be expressed as the net effect of the amount of the quantity being transported across the boundary by convection and diffusion and any sources or sinks within the control volume. The fluid is regarded as continuum, which assumes that the matter is continuously distributed in space [3].

In the derivation of the governing equations of fluid dynamics the Eulerian or control volume approach is conveniently used, rather than Lagrangian or material approach. Conservation equations represent the laminar flow of an incompressible Newtonian fluid. In some cases, additional processes take place and therefore, besides the basic equations, some additional transport equations have to be solved along with the mass and momentum equations.

The equations for the transport of a scalar variable can be written in the following form [3]:

$$\frac{\partial}{\partial t}\int_V \rho\phi dV + \int_S \left[\rho\phi\vec{v} - \Gamma_\phi\vec{\nabla}\phi\right]\cdot d\vec{S} = \int_V Q_{\phi,V}dV + \int_S \vec{Q}_{\phi,S}\cdot d\vec{S} \qquad (1)$$

where ϕ stands for the transported variable, Γ_ϕ is the diffusion coefficient and $Q_{\phi,S}$ and $Q_{\phi,V}$ stand for the surface exchange terms and volume sources, respectively. The momentum and energy equations can also be written in the form of (1). Equation (1) is therefore used as the generic equation for deriving the numerical procedure even though the momentum equation has to be treated as additional terms.

B. Conservation of Mass

The conservation equation of the continuity equation, for a control volume drive from (1) implies that the rate of change of the mass inside the control volume V is equal to the difference between inflow and outflow mass fluxes across the volume surface S. In integral form, the continuity equation can be written as:

$$\frac{\partial}{\partial t}\int_V \rho dV + \int_S \left[\rho\vec{v}\right]\cdot d\vec{S} = 0 \qquad (2)$$

where, ρ is the fluid density and $\vec{v}$ is the velocity. In incompressible flow, the first term in (2) is zero and the convection term cannot be ignored.

C. Conservation of Momentum

The conservation equation for momentum implies that the total variation of momentum, represented by the time variation of momentum within the control volume and the transfer of momentum across the boundary of the control volume by fluid motion, is caused by the net force acting on the fluid in the control volume.

$$\frac{\partial}{\partial t}\int_V \rho\vec{v}dV + \int_S \rho\vec{v}\vec{v}\cdot d\vec{S} = \int_S \sigma\cdot d\vec{S} + \int_V \rho f_b dV \qquad (3)$$

where σ is the stress tensor representing the surface forces and f_b represents the vector of body forces acting on the fluid. The stress tensor for Newtonian fluid can be expressed as:

$$\sigma = \mu\left[\vec{\nabla}\vec{v} + \left(\vec{\nabla}\vec{v}\right)^T\right] - pI \qquad (4)$$

where p is the pressure, μ is the dynamic viscosity of the fluid and I is the unit tensor. The vector (3) has to be resolved into specific directions resulting in three equations. The three equations are able to be solved independently.

D. Boundary Condition

To obtain the proper solutions, boundary conditions have to be specified at boundaries according to the type of equations. In general, the type of the boundary conditions can be classified into two groups: Dirichlet and Neumann boundary conditions.

Dirichlet boundary condition, when the value of a dependent variable at the boundary is specified,

$$\phi(r_b,t) = f(t). \qquad (5)$$

Neumann boundary condition, when the gradient of a dependent variable boundary is specified

$$\nabla\phi(r_b,t) = f(t). \qquad (6)$$

III. NUMERICAL METHOD

The FVM used in this study is based on a second-order accurate spatial discretization which accommodates

unstructured meshes with arbitrary-shaped cells. Computational points are located in the cell center and a segregated solution procedure is employed to solve the resulting set of non-linear algebraic equations. This leads to a decoupled system of linear algebraic equations for each dependent variable. The linearized equation systems are solved using a BICGSTAB solver. The SIMPLE algorithm for the pressure correction to satisfy the continuity equation is used to establish the pressure-velocity coupling.

A. Discretization

The computational domain is discretized by an unstructured mesh composed of a finite number of cells (control volume). Each control volume is bounded by a number of faces which compose the control volume surface. There is no restriction in the shape that the control volumes may have, i.e. an arbitrary polyhedral shape is possible as shown in Fig. 1. A data structure based on cell face is employed. It provides the data connectivity between the cells sharing the same cell face.
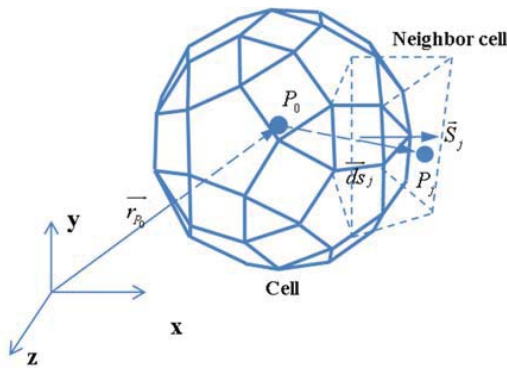

Fig. 1 Control volume of arbitrary shape.

First of all, the discretization procedures are applied for a Reynolds transport equation. The same procedure can be applied to the governing equations for fluid flow. When the Reynolds transport equation is integrated over a control volume, it will be appeared as:

$$\frac{\partial}{\partial t}\int_{V_0}\rho\phi dV + \sum_j\int_{S_j}\left[\rho\phi\vec{v} - \Gamma_\phi\vec{\nabla}\phi\right]\cdot d\vec{S}_j = \int_{V_0}Q_{\phi,V}dV + \sum_j\int_S\vec{Q}_{\phi,S}\cdot d\vec{S}_j \quad (7)$$

B. Convection Term

Convection term, which is the second term in LHS in (7) gives the rate at which variable ϕ_j enters or leaves the control volume through the cell face due to the mass flux F_j:

$$F_j = \int_{S_j}\rho\vec{v}\cdot d\vec{S} = (\rho\vec{v})_j\cdot\vec{S}_j \quad (8)$$

The velocity $\vec{v}_j$ at the CV face, needed for the evaluation of the mass fluxes, is obtained from an interpolation between two neighboring cell-center values.

The convective flux in (7) is approximated as:

$$C_j = \int_{S_j}\rho\phi\vec{v}\cdot d\vec{S} = F_j\phi_j \quad (9)$$

where F_j is the mass flux through the cell face j. One of the simplest is the linear interpolation, which provides the second-order accuracy. The value at the face center, which lies at the line connecting two neighboring cell centers, is obtained as:

$$\phi_j = \omega\phi_{P0} + (1-\omega)\phi_{Pj} \quad (10)$$

where ω is the interpolation factor calculated from distance between cell face and center point. Linear interpolation is usually referred to as central-differencing scheme (CDS) according to the geometry conditions. On the other hand, a widely used scheme, which guarantees bounded solutions (stable) is the upwind differencing scheme (UDS). The value of ϕ_j at cell-face center is approximated by the value at CV center on the upwind side of the face.

$$\phi_j = \begin{cases}\phi_{P0} & if & F_j \geq 0 \\ \phi_{Pj} & if & F_j < 0\end{cases} \quad (11)$$

UDS is unconditionally stable and it prevents the oscillatory solutions by scarifying accuracy. Since it is first-order scheme, UDS was found to be numerically very diffusive, requiring a very fine grid resolution to achieve acceptable accuracy.

To obtain the accuracy and the stability, the second-order CDS approximation can be blended with the first-order UDS approximation.

$$C_j = J_j\phi_j = J_j\phi^{UD} + \beta J_j\left(\phi^{CD} - \phi^{UD}\right) \quad (12)$$

where β is the blending factor with a value between zero and one. It is recommended to use the values of the blending factor as close to one as possible.

C. Diffusion term

The diffusion flux in (7) through the face j can be calculated as:

$$\int_{Sj}\Gamma_\phi grad\phi\cdot d\vec{S} \approx \sum_j\int_{Sj}\Gamma_\phi grad\phi\cdot d\vec{S} \approx \sum_j\Gamma_\phi\left(\nabla\phi\right)_j^*\cdot d\vec{S}_j = \sum_j D_j \quad (13)$$

where Γ_ϕ is the diffusion coefficient, which depends on each equation. In order to calculate the diffusion term on the cell face, an approximation of the derivative at the CV face is needed. This could be computed by interpolation of cell-center gradients to the cell-face center [6].

$$\left(\nabla\phi\right)_j^* = \left(\phi_{Pj} - \phi_{P0}\right)\frac{\vec{S}_j}{d\vec{s}_j\cdot\vec{S}_j} + \left[\overline{\nabla\phi_j} - \left(\overline{\nabla\phi_j}\cdot d\vec{s}_j\right)\frac{\vec{S}_j}{\vec{S}_j\cdot d\vec{s}_j}\right] \quad (14)$$

In (14), the first term on the RHS represents a central-difference approximation of the derivative in the

direction of a straight line connecting cells P_0 and P_j. This term is treated implicitly. The second term which corrects the error due to the fact that we need the derivative in the direction of cell-face normal direction is calculated using previous values of the variables and treated explicitly (source term).

D. Gradient at Cell Center

The gradient at the cell center can be calculated using Gauss theorem directly and mid-point rule.

$$\int_V grad\phi dV \approx \sum_j \phi_j d\vec{S}_j$$
$$\left(grad\phi\right)_{P0} = \frac{\sum_j \phi_j d\vec{S}_j}{V_{P0}} \qquad (15)$$

E. Algebraic Equation

By combining the approximations of all terms (convection, diffusion, source terms and so on), an algebraic equation for each CV is obtained.

$$A_{P0}\phi_{P0}^n + \sum_j^{nnb} A_{\phi j}\phi_{Pj} = b_\phi \qquad (16)$$

where the index j represents the neighbor nodes and b_ϕ contains source terms, contributions from the transient term, parts of convection and diffusion terms which are treated explicitly.

$$A_{\phi j} = -\Gamma_{\phi j}\frac{\left|\vec{S}_j\right|}{d\vec{s}_j} + \min(\dot{m}_j, 0) \qquad (17)$$

$$A_{\phi 0} = \sum\left[\max\left(\dot{m}_j, 0\right) + \Gamma\frac{\left|\vec{S}_j\right|}{\left|d\vec{s}_j\right|}\right] + \frac{(\rho V)_{P0}}{\delta t}$$

$$= -\sum_j A_{\phi j} + \sum_j J_j + \frac{(\rho V)_{P0}}{\delta t}$$

$$b_\phi = \sum_j \Gamma_{\phi j}\left[\overline{\nabla\phi_j}\cdot d\vec{S}_j - \left(\overline{\nabla\phi_j}\cdot d\vec{s}_j\right)\frac{\left|\vec{S}_j\right|}{\left|d\vec{s}_j\right|}\right]$$

$$-\sum_j \beta_\phi \dot{m}_j\left(\phi_j^{HD} - \phi_j^{UD}\right) + q_{\phi V} + q_{\phi S} + \frac{(\rho V)_{P0}^0}{\delta t}$$

IV. PRESSURE CALCULATION

The discretization procedures are applicable to the momentum and other transport equations for scalar quantities which can be represented in the form of the Reynolds transport equation. The difficulty to apply the procedures and obtain proper solutions is that there is no equation which contains the pressure as a dominant variable and thus, the pressure cannot be obtained directly. For compressible flows the density may be considered as a dependent variable which can be computed from the continuity equation, while the pressure can be obtained from an equation of state. In incompressible flow, the continuity equation is only an additional constraint on the velocity field which can be satisfied only by adjusting the pressure field. However, it is not obvious how this adjustment of pressure needs to be performed.

A. SIMPLE Algorithm

The SIMPLE method is based on an iterative procedure to satisfy the pressure constraint. Firstly, the linearized momentum equations are solved, using a known pressure of previous time step. The modified velocity field obtained from the momentum equation is used to calculate the continuity equation. Since the current velocity field does not satisfy the continuity equation, a mass residual will be produced. This value is then used to calculate the correction of pressure field. An appropriate equation between the velocity and pressure corrections is derived from the momentum equation. After the pressure correction, the velocities and pressure are updated. However, the new estimated velocities do not satisfy momentum equation, and thus, the iterative procedure is continued until both the momentum and the continuity equations are satisfied.

Since collocated variable arrangement is used, a simple linear interpolation (second order difference) of velocity can lead to oscillations in the pressure field. In order to avoid oscillations of solutions, a special interpolation is required. It implies that the cell face velocity depends not only on the velocity field but also on the pressure field. The third-order pressure diffusion term is added to the velocity, which does not scarify the accuracy.

$$\vec{v}_j^* = \vec{v}_j + \delta\vec{v}_j \qquad (18)$$

$$\delta\vec{v}_j = -\overline{\left(\frac{V_0}{A_{v0}}\right)_j}\left[\frac{p_{Pj} - p_{P0}}{d\vec{s}_j\cdot\vec{n}} - \frac{\overline{\nabla p\cdot d\vec{s}_j}}{d\vec{s}_j\cdot\vec{n}}\right]\frac{\vec{S}_j}{\left|\vec{S}_j\right|}$$

$$\overline{\left(\frac{V_0}{A_{v0}}\right)_j} = \frac{V_{P0} + V_{Pj}}{A_{vP0} + A_{vPj}}$$

where overbar denotes the arithmetic average of the values at cell P_o and P_j.

B. Pressure Correction

By employing the SIMPLE algorithm [6], the correction of the mass flux through the cell face can be expressed in term of the gradient of the pressure correction and the final pressure correction equation of incompressible flow can be obtained as:

$$A_{P0}p_{P0}' + \sum_j^{nnb} A_{Pj}p_{Pj}' = b_{P0} \qquad (19)$$

$$p_{Pj}' = -\rho_j^*\overline{\left(\frac{V_{P0}}{A_{v0}}\right)_j}\frac{\left|\vec{S}_j\right|}{\left|d\vec{s}_j\right|}$$

$$p_{P0}' = -\sum_j A_{Pj}$$

$$b_{P0} = -\sum_j J_j^*$$

where super script * implies the value which satisfy the

momentum equation. After solving the equation, the pressure-correction process is used to correct and update pressure and velocity fields and mass fluxes.

$$p = p^* + \beta_p p'$$ (20)

$$\vec{v} = \vec{v}^* + \vec{v}' = \vec{v}^* - \frac{V_0}{A_{v0}}(\nabla p')_{P0}$$

$$J_j = J_j^* + J_j' = J_j^* + A_{Pj} p'_{Pj} - A_{Pj} P'_{P0}$$

where β_p is an under-relaxation factor, which is necessary because the calculated pressure-correction is usually overestimated due to simplifications. The general value of under-relaxation factor β_p are 0.1 to 0.3 for steady problems. In unsteady, it can be chosen up to 1 [3].

V. RESULTS AND DISCUSSION

A. Lid Driven Cavity

Lid-driven-cavity flow has been a test and validation problem for the viscous codes developed in this study. Its elliptic and nonlinear nature, which is common in general engineering problem is the characteristics of the problem, and provides a good test of the computational procedure. In addition, the simple geometry is another advantage. The configuration used in this study is showing in Fig. 2.
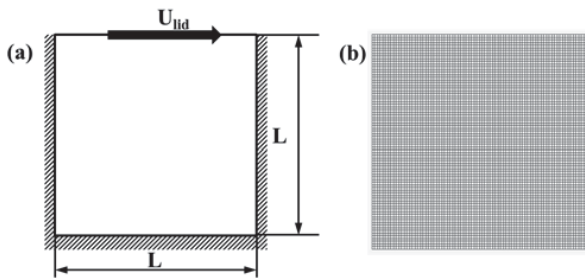

Fig. 2 (a) Geometry and (b) grid of lid driven cavity

The velocity at the top of the cavity is set at 1 unit velocity (typically 1 m/s). The cavity is a square and its height and width are unit dimensions (typically 1 m). The other three boundaries are viscous walls, which are non-slip boundaries. The Reynolds number is defined by height or width and velocity at the top.

$$Re = \frac{\rho U_{lid} L}{\mu}$$ (21)

where ρ is the density, U_{lid} is the speed of the top wall boundary, L is the length of square cavity, and μ is the viscosity of the fluid. Flow at Reynolds number of 100, 400 and 1000, is simulated and compared with results of [7].

The uniform and square grid is used in this numerical simulation, as shown in Fig. 2. The unstructured grid has one layer of z direction for two-dimensional flow. The fully-implicit scheme is used with considerably large time step (1×10^{15}) for steady state. Oscillations of the residuals of mass and momentum equations are observed at a short initial period when the flow is under development. Fig. 3 shows the u-velocity profile along the centerline, and the v-velocity profile along the horizontal centerline. The more refined mesh gives a more accurate profile than the coarser mesh in Fig. 3 (c).

Fig. 4 shows streamlines of the three Reynolds numbers. The streamlines from the present analysis can be seen in a right hand side in Fig. 4. The streamline profiles match well with that of previous study [7] in left hand side. The main vortex is slightly off center, closer to the upper right corner when the Reynolds number is 100. Two single vortices are observed at the left and right lower corners of the cavity. The size of the right vortex is slightly larger than that of the left one.

The center of the vortex core at Re=400, the main circular flow is centered about a point which is slightly above and to the right of the center of the cavity as show in Fig. 4. The large secondary vortex at the lower right can be observed than Re=100. The streamlines in case of Re=1000 shows the same structure as that of the Re=400. Some small changes are observed in the size and location of the vortexes as shown in Fig. 4 (c).
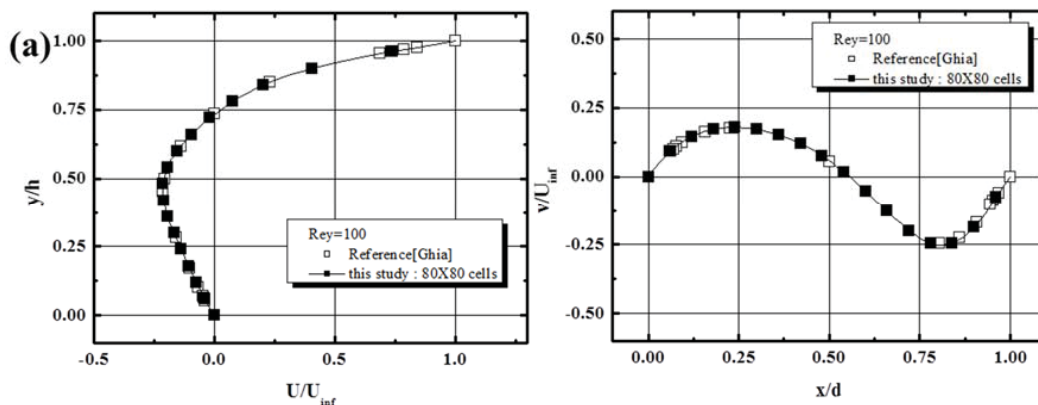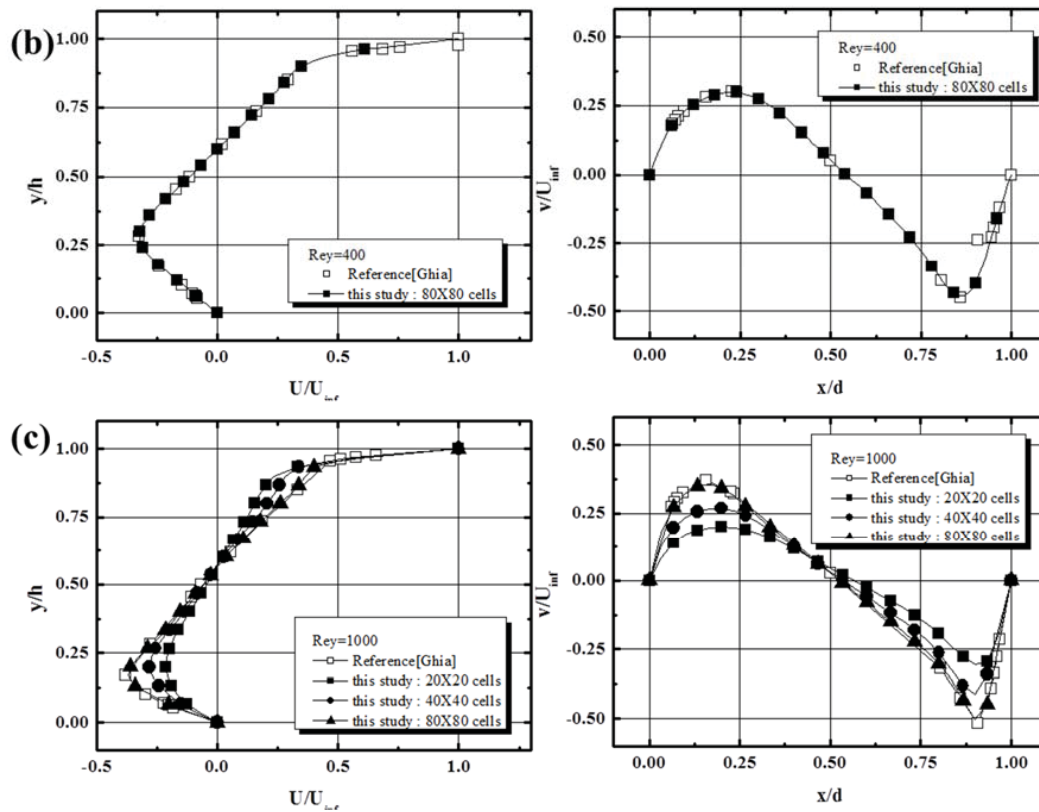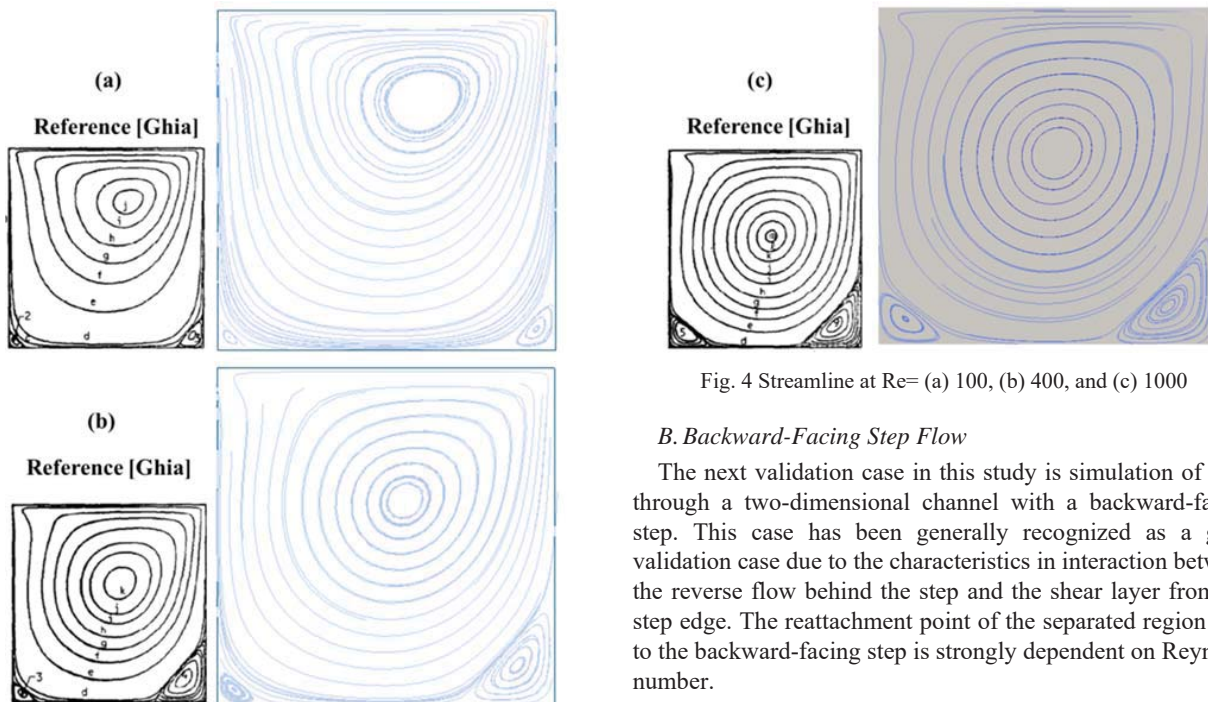
Fig. 3 *u* and *v* velocity at Re= (a) 100, (b) 400, and (c) 1000

Fig. 4 Streamline at Re= (a) 100, (b) 400, and (c) 1000

B. Backward-Facing Step Flow

The next validation case in this study is simulation of flow through a two-dimensional channel with a backward-facing step. This case has been generally recognized as a good validation case due to the characteristics in interaction between the reverse flow behind the step and the shear layer from the step edge. The reattachment point of the separated region next to the backward-facing step is strongly dependent on Reynolds number.
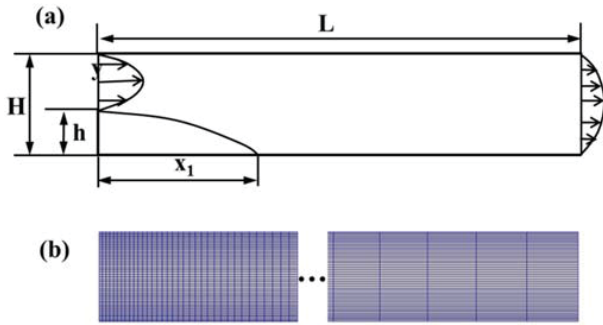
Fig. 5 Backward-facing step of (a) geometry and (b) grids

Fig. 5 shows a schematic view of a backward-facing step channel and a grid used in this study. The length of the total channel, L, is 20 unit lengths. The inlet of the channel at the right hand side is heights of 0.5 units while the overall height of the channel, H, is 1 unit. The expansion ratio, which is defined as the ratio of the height of the channel to the inlet height is 2. In some studies, the expansion ration is used as 1.94 [8]. In this study, the expansion ratio of two is used. There is ignorable difference of results between 2 and 1.89 of expansion ratio [8], [9]. We directly compare the results between experimental [8] and computation results in this study.

The profile of the velocity entering the channel is set to the velocity profile of fully developed two-dimensional channel flow. It is a parabolic profile for the x-directional velocity component u.

$$u = V_{avg}\left(1-\left(\frac{y}{H-h}\right)^2\right) \tag{22}$$

where the constant V_{avg} is average velocity along the inlet. In this study, the average velocity of the inflow across the inlet is set to 1 unit velocity. There cases were tested for Reynolds numbers of 100, 389, and 1000. The Reynolds number for this problem is defined by:

$$Re = \frac{\rho V_{avg} H}{\mu} \tag{23}$$

In the Reynolds numbers of 100, and 389, the steady state solver with a considerably large time is used and we obtain stable and converged solutions. However, in the Reynolds number of 1000, we use fully implicit method with a time step size 0.1 because of the stability problem. After 20 unit time, the residual (relative error) is reduced to under 1×10^{-4}.
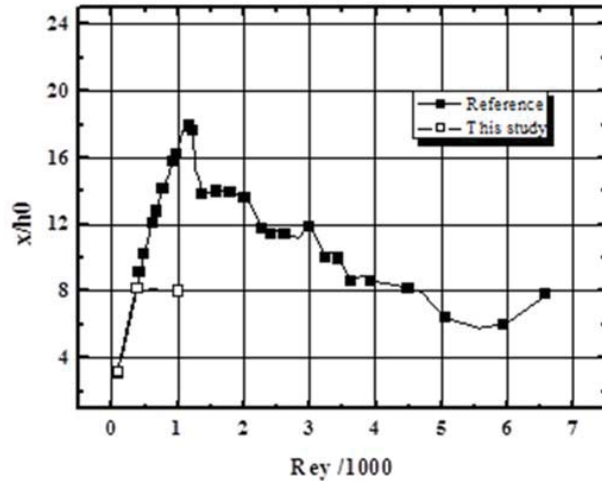

Fig. 6 Location of reattachment as function of Reynolds numbers

The flow is laminar when the Reynolds number is less than 1200, while the flow is two-dimensional when the Reynolds number is less than 400 [8]. In Fig. 6, the reattachment points move downstream as the Reynolds number increases from 100 to 400, and thus the CFD results of this study agree well with experimental results. However, at Re=1000, the differences are quite large because of its three-dimensional effects. The similar differences can be found in Fig. 7. The developing flow and reattachment point after backward-facing step is properly predicted.

VI. Conclusions

In this study, the numerical algorithms for incompressible Navier-Stokes flow on unstructured grids with arbitrary shaped cells have been developed. Third order diffusion method is chosen to avoid the checkerboard pressure oscillation generally encountered in a collocated method for solving incompressible flow. The numerical algorithm used to solve the final linear equations is derived from the SIMPLE algorithm. The numerical models used in this study have been validated using two typical validation problems such as the lid-driven cavity and the backward-facing step channel. A good agreement with existing experimental data and numerical data is obtained for all cases except high Reynolds flow (1000) of a backward-facing step because of its three-dimensional effect. Even though the accuracy of the solution is acceptable, the convergence of the numerical code developed in this study is still slow because of some abundant processes in it. It is required a code optimization and acceleration techniques such as local time step, arithmetic multi-grid methods and so on.
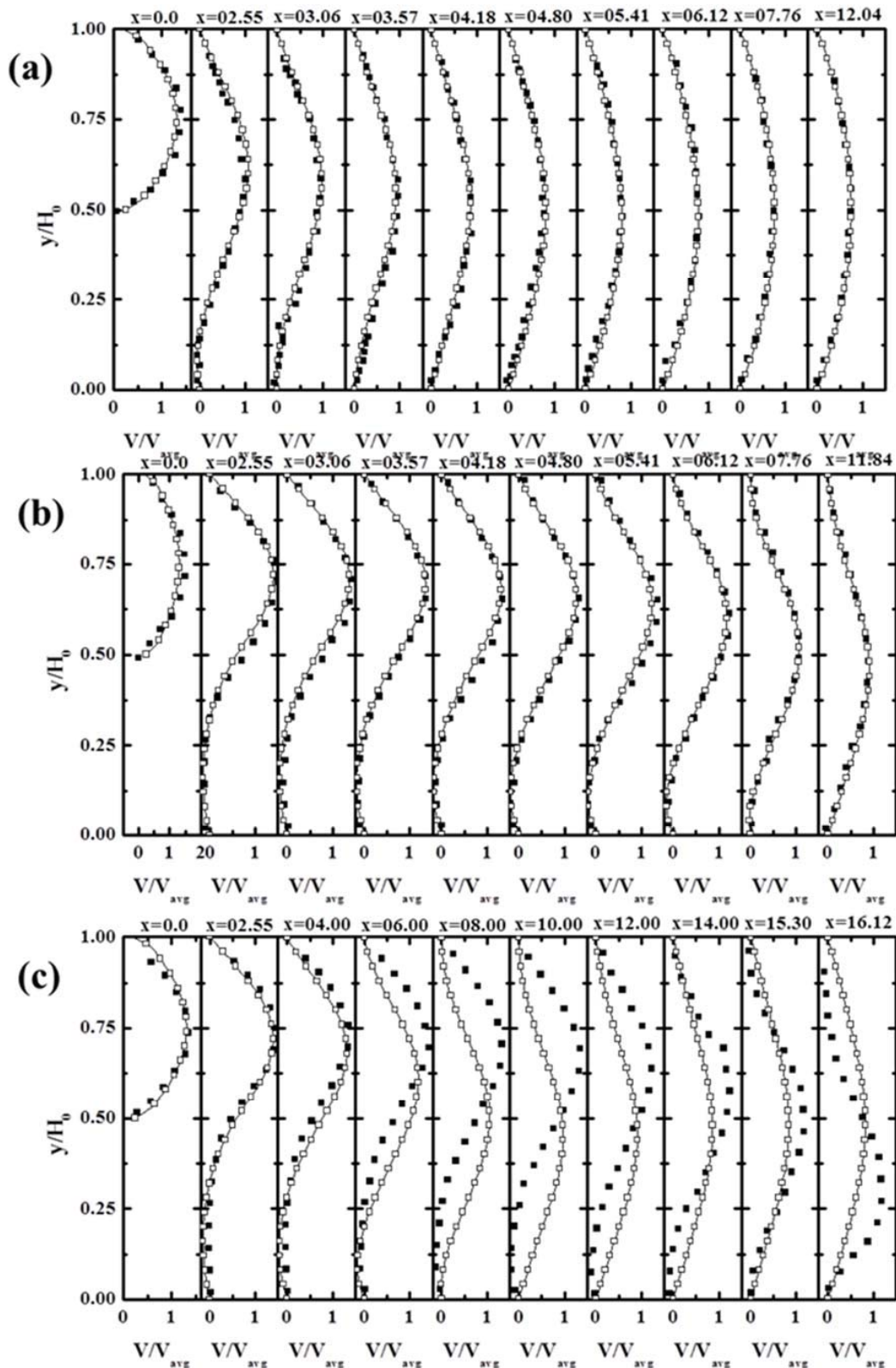
Fig. 7 Velocity profile for Re=100, 389, and 1000 along the channel: filled squires from Reference 8, and hollow square- this study

REFERENCES

[1] Samir Muzaferija, *Adaptive Finite Volume Method for Flow Prediction using Unstructured Meshes and Multigrid Approach*, Ph.D. thesis, Imperial College, 1994.
[2] Angela Lestari, *Development of unsteady algorithms for pressure-based unstructured solver for two-dimensional incompressible flows*, Master Thesis, Iowa State University, 2009.
[3] Hidajet HADZI, *Development and Application of a Finite Volume Method for the Computation of Flows Around Moving Bodies on Unstructured, Overlapping Grids*, Ph. D thesis, Technical University of Hamburg- Harburg, 2005.
[4] Mathur, S. R., and Murthy, J. Y., "A Pressure-based Method for Unstructured Meshes," *Numerical heat transfer, part B*, Vol. 31, No. 2, pp. 195-215, 2007.
[5] Patankar, S. V., *Numerical Heat Transfer and Fluid Flow*, Hemisphere Publishing Corp, New York, 1980.
[6] Ferziger, J. H., Peric, M., *Computational Methods for Fluid Dynamics,* Springer Verlag Berlin Heidelberg, 1996.
[7] Ghia, U. Ghia, K. N., and Shin, T., "High-Re Solutions for Incompressible Flow Using the Navier-Stokes Equations and a Multigrid Method," *Journal of Computational Physics*, Vol. 48, pp. 387-411, 1982.
[8] Armaly, B. F., Pereira J. C. F., Schonung, B., "Experimental and theoretical investigation of backward-facing step flow," *J. Fluid Mech.,* Vol. 127, pp. 473-496, 1983.
[9] Wirogo, S., *Flux Corrected Method: An Accurate Approach to Fluid Flow Modeling*, Ph. D thesis, Iowa State University, Ames, 1997.

Juhee Lee finished his Ph.D. at Hanyang Univerty in Seoul Korea. The title of his Ph.D. paper is the pareto optimization of WIG airfoil based on the multi-objective genetic algorithm. His specialty is analysis and design ground effect vehicle considering optimal wing shape. Optimal method used in his research is a genetic algorithm for multiple objectives. The final optimum is a set of pareto. Through the analysis of the pareto optimum, the system can be identified. He is working at Hoseo University after industrial experience at CD-Adapco Korea for 5 years. Prof. Lee is member of Korean society of mechanical engineering, Korean society for aeronautical and space sciences, and Korea Institute of Ecological architecture and environment.

Yongjun Lee finished his Ph. D at Yonsei University in Seoul Korea. The title of his Ph.D. paper is A study on the operational strategy for hybrid ventilation system in apartment unit focused on indoor air quality. He is working at BEL Technology Co., Ltd. as CEO. Dr. Lee is member of The Architectural Institute of Korea, The Society of Air-conditioning and Refrigerating Engineers of Korea, and Korea Institute of Ecological Architecture and Environment